BRIEF REPORT

Zika Virus Infection with Prolonged Maternal Viremia and Fetal Brain Abnormalities

R.W. Driggers, C.-Y. Ho, E.M. Korhonen, S. Kuivanen, A.J. Jääskeläinen, T. Smura, A. Rosenberg, D.A. Hill, R.L. DeBiasi, G. Vezina, J. Timofeev, F.J. Rodriguez, L. Levanov, J. Razak, P. Iyengar, A. Hennenfent, R. Kennedy, R. Lanciotti, A. du Plessis, and O. Vapalahti

SUMMARY

The current outbreak of Zika virus (ZIKV) infection has been associated with an apparent increased risk of congenital microcephaly. We describe a case of a pregnant woman and her fetus infected with ZIKV during the 11th gestational week. The fetal head circumference decreased from the 47th percentile to the 24th percentile between 16 and 20 weeks of gestation. ZIKV RNA was identified in maternal serum at 16 and 21 weeks of gestation. At 19 and 20 weeks of gestation, substantial brain abnormalities were detected on ultrasonography and magnetic resonance imaging (MRI) without the presence of microcephaly or intracranial calcifications. On postmortem analysis of the fetal brain, diffuse cerebral cortical thinning, high ZIKV RNA loads, and viral particles were detected, and ZIKV was subsequently isolated.

Zika virus (ZIKV), a mosquito-borne flavivirus and member of the Flaviviridae family, was originally isolated from a sentinel primate in Uganda in 1947.[1] ZIKV was associated with mild febrile disease and maculopapular rash in tropical Africa and some areas of Southeast Asia. Since 2007, ZIKV has caused several outbreaks outside its former distribution area in islands of the Pacific: in 2007 on Yap island in Micronesia, in 2013 and 2014 in French Polynesia, and in 2015 in South America, where ZIKV had not been identified previously.[2-5] There are separate African and Asian lineages of the virus,[6] and the latter strains have caused the outbreaks in the Pacific and the Americas.[7] As in the transmission of dengue and chikungunya viruses, the main transmission cycle of ZIKV occurs between urban aedes mosquitoes and humans.

One striking feature of the current ZIKV outbreak is the apparent increased risk of intrauterine or perinatal transmission of the virus as well as the marked increase in the number of newborns with microcephaly reported in Brazil.[8-17] A recent prospective study showed fetal ultrasonographic abnormalities in 12 of 42 women (29%) with ZIKV infection during pregnancy; 7 of the 42 fetuses (17%) that were studied had microcephaly, cerebral atrophy, or brain calcifications.[11] Because of the association between ZIKV infection and microcephaly and other neurologic disorders, the World Health Organization has declared the ZIKV epidemic a public health emergency of international concern.[13]

Early in this particular outbreak, investigations into the viral pathogenesis, vertical transmission rates, potential viral cofactors, and sensitivity and specificity of diagnostic testing have presented more questions than answers. Nevertheless,

The authors' full names, academic degrees, and affiliations are listed in the Appendix. Address reprint requests to Dr. Driggers at rdrigge1@jhmi.edu, to Dr. du Plessis at adupless@childrensnational.org, or to Dr. Vapalahti at olli.vapalahti@helsinki.fi.

Drs. Driggers and Ho, Ms. Korhonen, and Ms. Kuivanen and Drs. du Plessis and Vapalahti contributed equally to this article.

This article was published on March 30, 2016, at NEJM.org.

DOI: 10.1056/NEJMoa1601824

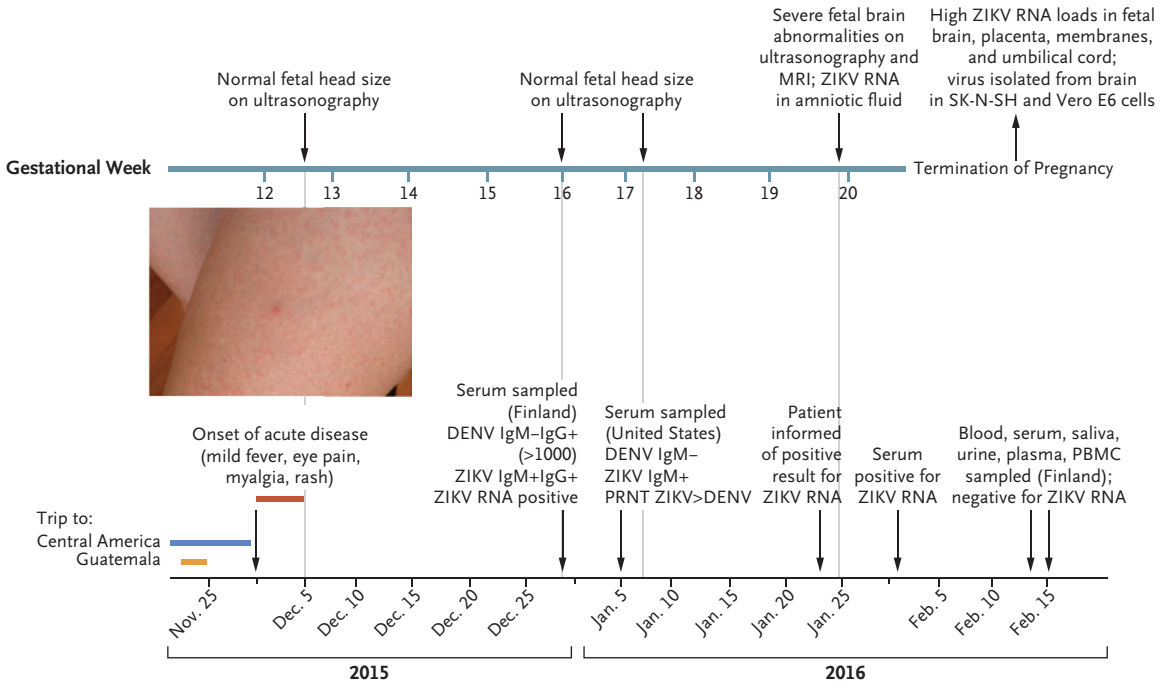

Figure 1. Timeline of Symptoms and Radiographic and Laboratory Studies.

This timeline highlights the symptoms of Zika virus (ZIKV) infection in the mother (bottom row) and the corresponding radiographic and laboratory findings in the fetus (top row). The inset photograph shows the mother's rash at the time of the onset of the acute illness. DENV denotes dengue virus, MRI magnetic resonance imaging, PBMC peripheral-blood mononuclear cells, and PRNT plaque-reduction neutralization test.

the Centers for Disease Control and Prevention (CDC) has issued a travel advisory for pregnant women,[15] as well as guidelines for health providers caring for all travelers from affected regions.[16,17] The CDC recommends that pregnant women with a history of travel to an area in which ZIKV is endemic should undergo ZIKV serologic testing and fetal ultrasonography to screen for microcephaly or intracranial calcifications.[16] For a diagnosis of fetal ZIKV infection, RNA detection in amniotic fluid may be considered in pregnant women with positive results on ZIKV serologic testing.[16] Here we present a report of a case of congenital ZIKV infection and subsequent findings in a pregnancy that was terminated at 21 weeks of gestation.

CASE REPORT

A 33-year-old Finnish woman who was in the 11th week of gestation was on holiday in Mexico, Guatemala, and Belize with her husband in late November 2015. (Details are provided in Section 1.0 of the Supplementary Appendix, available with the full text of this article at NEJM.org.) During their travels, she and her husband recalled being bitten by mosquitoes, particularly in Guatemala. One day after her arrival at her current residence in Washington, D.C., she became ill with ocular pain, myalgia, and mild fever (maximum, 37.5°C), which lasted for 5 days. On the second day of fever, a rash developed (Fig. 1, and Fig. S5 in the Supplementary Appendix). Her husband was concomitantly reporting similar symptoms. Serologic analysis that was performed 4 weeks after the onset of illness while she was on a trip to her native Finland was positive for IgG antibodies and negative for IgM antibodies against dengue virus. Subsequent serologic analysis was positive for both IgG and IgM antibodies against ZIKV, findings that were compatible with acute or recent ZIKV infection. Serologic analysis for the presence of chikungunya virus was negative. The patient had been vaccinated against tick-borne

encephalitis and yellow fever more than 10 years earlier.

Fetal ultrasonography that was performed at 13, 16, and 17 weeks of gestation (1, 4, and 5 weeks after the resolution of symptoms) showed no evidence of microcephaly or intracranial calcifications. However, there was a decrease in the fetal head circumference from the 47th percentile at 16 weeks to the 24th percentile at 20 weeks.

At 16 weeks of gestation, the presence of flavivirus in serum was detected on nested reverse-transcriptase–polymerase-chain-reaction (RT-PCR) assay, and sequencing showed identity to Central American epidemic strains of ZIKV. The finding was confirmed with a specific ZIKV quantitative RT-PCR assay (Table S2 in the Supplementary Appendix). The Division of Vector-Borne Diseases Arbovirus Diagnostic Laboratory at the CDC reported serologic evidence of infection at 17 weeks of gestation, with serum positivity for ZIKV IgM and a titer of more than 1:2560 on a plaque-reduction neutralization test. On the basis of these results, the patient sought more thorough assessment of the fetus.

Fetal ultrasonography at 19 weeks of gestation showed abnormal intracranial anatomy (Fig. 2, and Fig. S1 in the Supplementary Appendix). The cerebral mantle appeared to be thin with increased extra-axial spaces. Both frontal horns were enlarged with heterogeneous, predominantly echogenic material present in the frontal horn and body of the left lateral ventricle, a finding that raised concern about intraventricular hemorrhage. Dilation and upward displacement of the third ventricle, dilation of the frontal horns of the lateral ventricles, concave medial borders of the lateral ventricles, and the absence of the cavum septum pellucidum suggested agenesis of the corpus callosum. No parenchymal calcifications were seen. The head circumference measured in the 24th percentile for gestational age. The remainder of the fetal anatomy was normal.

Fetal MRI at 20 weeks of gestation showed diffuse atrophy of the cerebral mantle, which was most severe in the frontal and parietal lobes, with the anterior temporal lobes least affected (Fig. 3). The normal lamination pattern of the cerebral mantle was absent, and the subplate zone was largely undetectable. The corpus callosum was significantly shorter than expected for gestational age, with an anterior–posterior length of 14 mm (expected range, 18 to 22).[18,19] The cavum septum pellucidum was very small. The lateral ventricles were mildly enlarged, as was the third ventricle, with a transverse diameter measuring 2.5 mm (average measurement at gestational age, 1.75 mm [range, 1.1 to 2.3]).[18] The fourth ventricle was normal. The volume of the choroid plexus was unusually prominent, without evidence of hemorrhage. No focal destructive lesions were identified within the cerebral cortex or white matter. The cerebellum was normal in appearance and size. Given the grave prognosis,

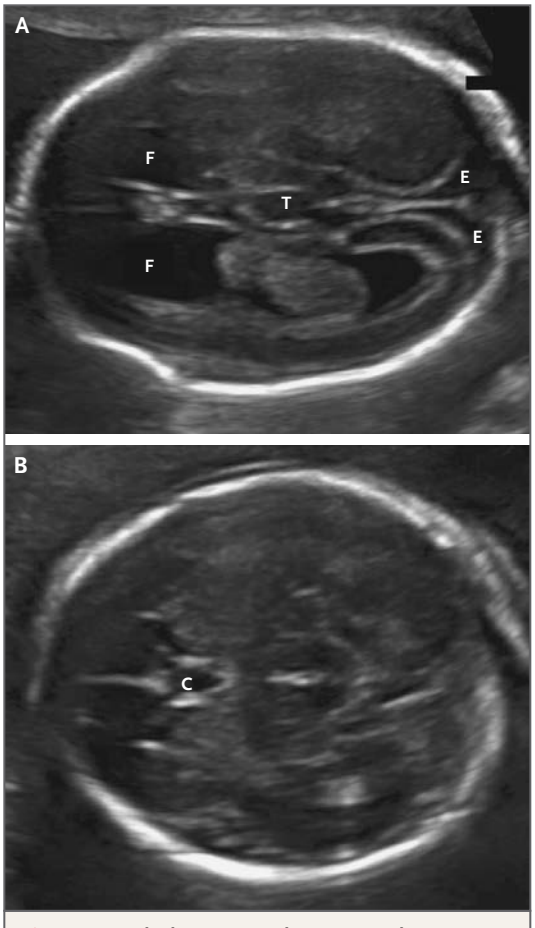

Figure 2. Fetal Ultrasonography at 19 Weeks of Gestation.

In an ultrasonographic image of the brain of the ZIKV-exposed fetus in this report (Panel A), shown are a thin cerebral cortex with increased extra-axial space (E), dilation of the third ventricle (T), enlargement of both frontal horns (F), and the apparent absence of the cavum septum pellucidum, as compared with an image obtained in a normal fetus of the same gestational age with a visible cavum septum pellucidum (C) (Panel B).

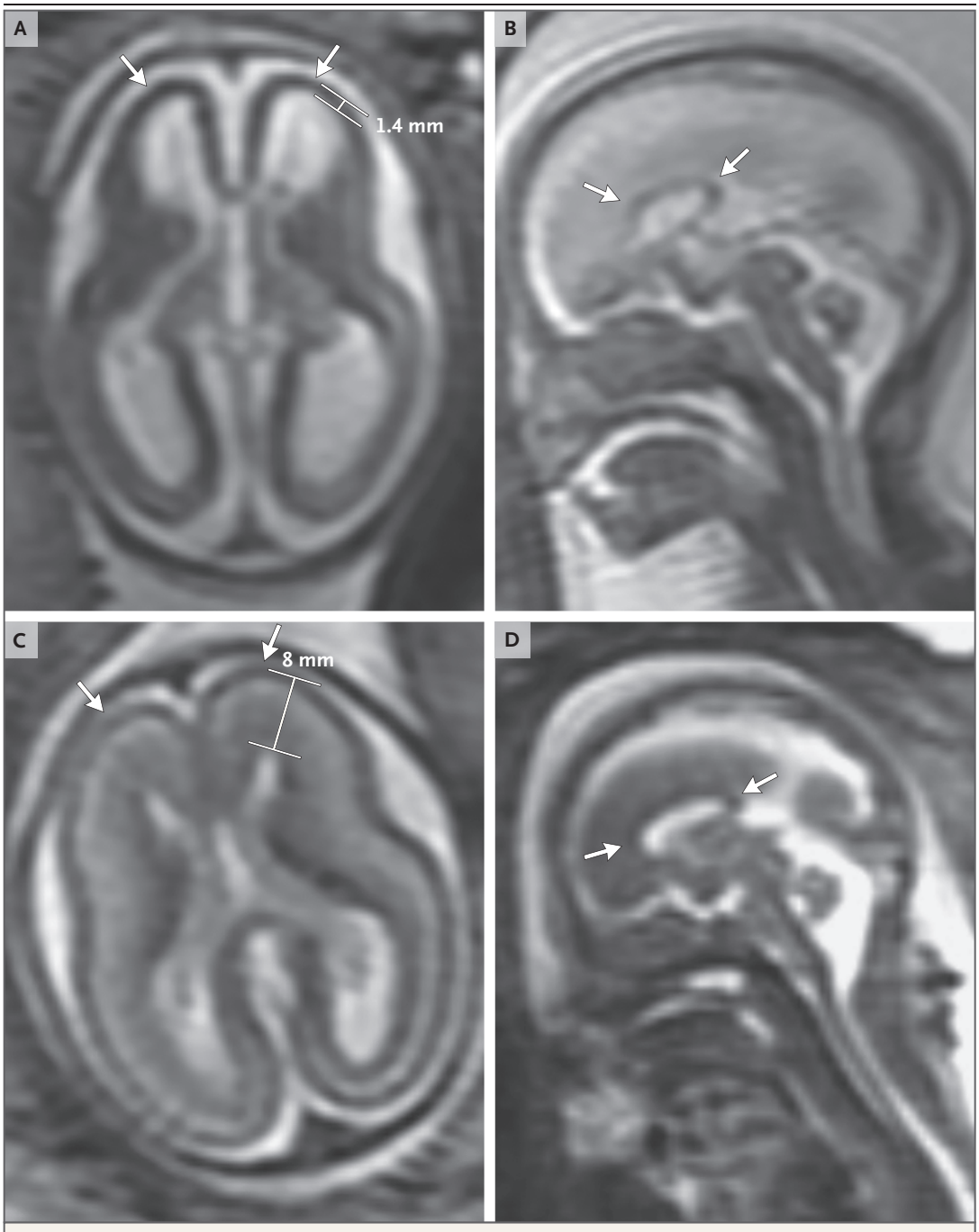

Figure 3. Magnetic Resonance Imaging of the Fetal Brain at 19 Weeks of Gestation.

On T_2-weighted imaging of the brain of the ZIKV-exposed fetus, a 3-mm-thick axial view (Panel A) shows severe atrophy of the cerebral mantle, which was most visible in the frontal regions (arrows) where the cortical mantle measures 1.4 mm. In a 2-mm-thick midline sagittal image (Panel B), the small corpus callosum (arrows) is visible, with an anterior–posterior length of 14 mm (normal range, 18 to 22).[18,19]. Below are matching images of the same locations and thicknesses in a normal fetus with a gestational age of 20 weeks 3 days, showing the cortical mantle measuring 8 mm (in Panel C) and the corpus callosum measuring 20 mm (in Panel D).

the patient elected to terminate the pregnancy at 21 weeks of gestation.

METHODS

We tested samples obtained from the patient, her spouse, and the fetus and from viral isolation trials for ZIKV RNA using nested pan-flavivirus RT-PCR and quantitative RT-PCR for ZIKV. Levels of ZIKV IgM, IgG, and neutralizing-antibody titers were determined by means of standard methods. We performed immunohistochemical and electron microscopic analyses to study fetal brain tissue. Viral isolation trials using the patient's serum and fetal tissues were performed with the use of SK-N-SH human neuroblastoma cells, Vero E6 green monkey kidney cells, and C6/36 *Aedes albopictus* mosquito cells. We used next-generation sequencing and Bayesian analysis to study the genetics of the ZIKV strain isolate. Additional details about the analyses are provided in the Methods section of the Supplementary Appendix.

RESULTS

FETAL NEUROLOGIC ABNORMALITIES

A postmortem examination was performed with materials collected for additional study. Gross examination showed normal fetal anatomy and severe autolysis. The brain weighed 30 g (reference weight, 49±15[20]) and showed no apparent gross abnormalities. Microscopic analysis revealed abundant apoptosis primarily affecting the intermediately differentiated postmigratory neurons in the neocortex (Fig. 4, and Fig. S2 in the Supplementary Appendix). Early mineralization was seen in association with apoptotic neurons focally. In contrast, the well-differentiated neurons of the basal ganglia and limbic regions as well as primitive cells in the germinal matrix appeared to be unaffected.

In addition to the cortical neuronal abnormalities, the subventricular zone and white matter showed severe volume loss with extensive axonal rarefaction and macrophage infiltrates (Fig. 4). This pattern correlates with the atrophy of the subplate seen on prenatal imaging. There was diffuse infiltration of macrophages in the cerebral cortex, subventricular zone, white matter, and leptomeninges but not in the germinal matrix of the ganglionic eminence. Scattered loose microglial aggregates were observed in the deep gray matter and brain stem, but there was no evidence of well-formed microglial nodules or other classic histologic features of viral encephalitis, such as perivascular inflammatory infiltrates, viral inclusions, or ventriculitis. Ultrastructural examination of fixed cortical tissue showed a rare aggregate of intracellular electron-dense, viral-like particles that measured 39 to 41 nm in diameter (mean, 40.26). Our ability to specifically localize the cellular compartment housing the particles was limited by poor tissue preservation, but the morphologic features and size of this structure were similar to those reported by Mlakar et al.[10] and the CDC.[21] The choroid plexus was focally enlarged and edematous, with scant hemosiderin deposits, which may appear to be similar to intraventricular hemorrhage on prenatal imaging. Histologic examination of the eyes, spinal cord gray matter, dorsal-root ganglia, and spinal nerves did not reveal overt microscopic abnormalities. Spinal white-matter tracts were not well visualized. A detailed pathological description of the brain and other organs is provided in the Methods section of the Supplementary Appendix.

FETAL AND MATERNAL ZIKV VIRAL LOADS

The highest ZIKV viral loads were found in fetal brain, with substantial viral loads in the placenta, fetal membranes, and umbilical cord, as studied on quantitative RT-PCR (Table S2 in the Supplementary Appendix). Lower amounts of ZIKV RNA were found in fetal muscle, liver, lung, and spleen. Amniotic fluid that was obtained at the time of termination was positive for ZIKV RNA with low viral counts. On PCR assays to detect DNA, the amniotic fluid was negative for parvovirus B19, herpes simplex virus types 1 and 2, cytomegalovirus (CMV), and *Toxoplasma gondii*, and the fetal brain tissue was negative for herpes simplex virus types 1 and 2 and varicella–zoster virus.

Maternal serum that was obtained on the day before termination was also positive for ZIKV RNA with a low viral count (2.1×10^3 copies per milliliter). No ZIKV RNA was detected in the serum, peripheral-blood mononuclear cells, saliva, or urine in samples obtained 11 days and 13 days after termination. On IgM analysis, the mother had no evidence of serum antibodies indicating acute infection with CMV, parvovi-

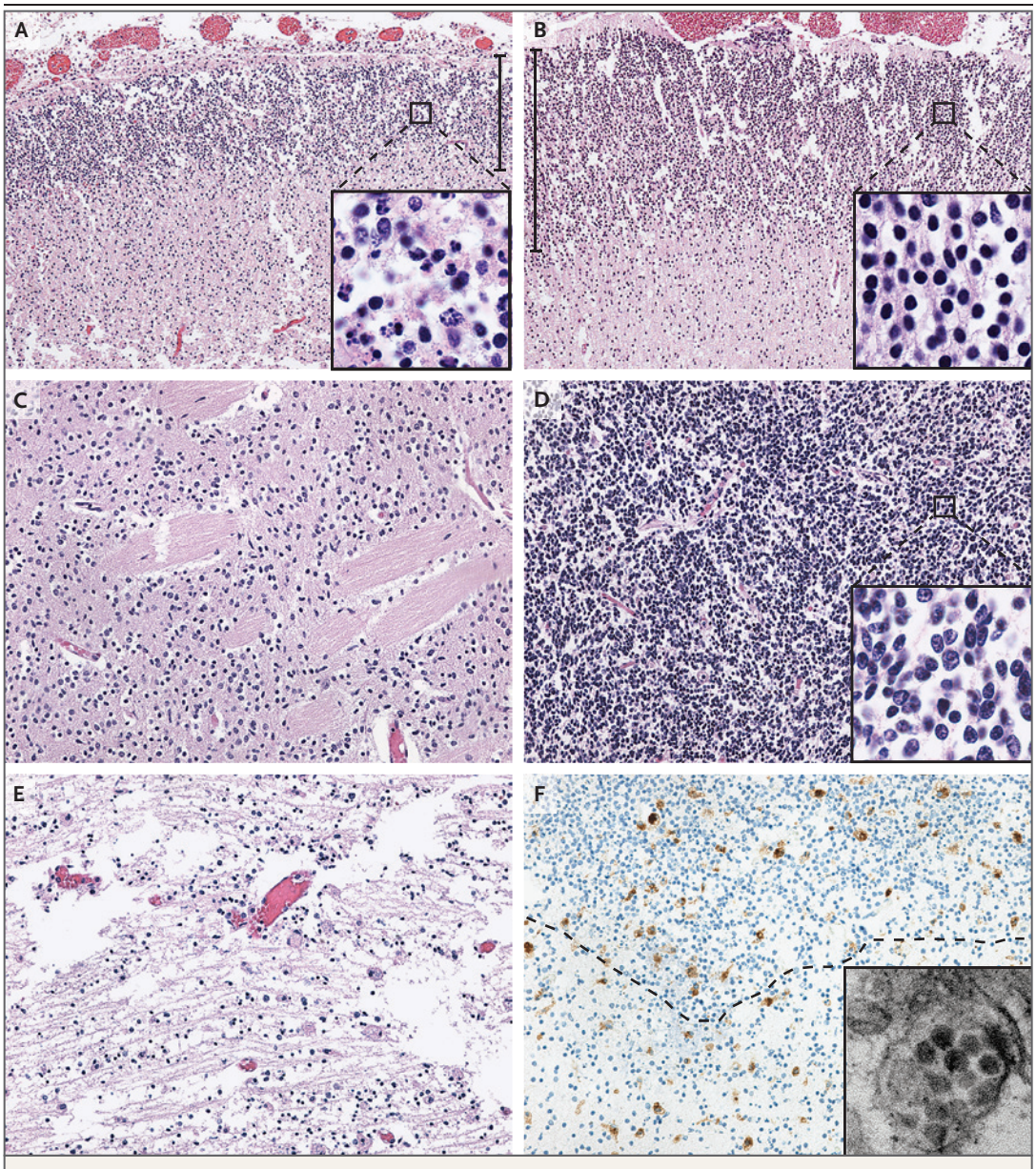

Figure 4. Neuropathological Features of Fetal ZIKV Infection.

In postmortem analyses of samples obtained from the fetus, an area of parietal cortex has abundant apoptotic neurons (Panel A), with detail shown in the inset view. The unaffected occipital cortex is thicker than the parietal cortex (Panel B), as indicated by the vertical bars. The basal ganglia (striatum) appears to be morphologically normal (Panel C), and cells in the germinal matrix of the ganglionic eminence are histologically normal (Panel D). White matter shows extensive axonal rarefaction and infiltrates of macrophages containing foamy cytoplasm and cellular debris in some cells (Panel E) (hematoxylin and eosin staining in Panels A through E). Panel F shows macrophage infiltrates in the cortex (area above the dashed line) and subcortical white matter (area below the dashed line) (anti-CD68 immunostaining with hematoxylin counterstaining). The inset shows possible viral-like particles within a subcellular compartment, as seen on electron microscopy.

rus B19, *T. gondii*, or rubella virus. Samples obtained from her spouse were all negative for ZIKV RNA, including urine (obtained 11 weeks after travel), serum (obtained 5 and 11 weeks after travel), and semen (obtained 10 and 12 weeks after travel), although results of testing for ZIKV IgG (titer 320) and IgM (titer 20) were positive.

VIRUS ISOLATION

ZIKV replication was detected as an increase in ZIKV RNA on quantitative RT-PCR assay of SK-N-SH and Vero E6 cells inoculated with the fetal brain sample. The quantities of ZIKV RNA increased rapidly in the SK-N-SH cells after the first day of inoculation, whereas in the Vero E6 cells, viral RNA loads started to increase on day 4 after inoculation. Viral replication was not detected in cells inoculated with other samples. The tissue-inoculated SK-N-SH and Vero E6 cells were further shown to express ZIKV antigens by reactivity with human convalescent anti-ZIKV serum (obtained from the father of the fetus) on immunofluorescence staining and to produce flavivirus-like particles, as seen on electron microscopy (Fig. 5).

A complete ZIKV genome was sequenced from supernatant of SK-N-SH cells on day 5 after inoculation. Phylogenetic analysis indicated that the viral strain (designated ZIKV_FB-GWUH-2016; GenBank number, KU870645) was a member of the Asian genotype and closely related to two ZIKV sequences obtained from Guatemalan patients who presented with mild illness (Fig. 6, and Fig. S6 in the Supplementary Appendix).[7] The FB-GWUH-2016 strain had 23 to 51 nucleotide differences and 8 to 14 amino acid differences as compared with the ZIKV strains detected previously in the Americas (99.6 to 99.8% identities) (Fig. 5D). Five of the eight differences in amino acids between FB-GWUH-2016 and the Guatemalan strains were specific for the FB-GWUH-2016 strain (i.e., differences that were not detected in other ZIKV strains sequenced so far). One amino acid substitution was a reversion toward the African ZIKV genotype. Three amino acid substitutions were common for FB-GWUH-2016 and the Guatemalan strains but distinct from all other reported ZIKV strains.

DISCUSSION

The current recommendations for ZIKV diagnostic practices are based on the understanding that ZIKV viremia lasts for less than a week after the onset of infection.[15] During the week of symptomatic infection, RNA detection in serum or blood is considered to be the diagnostic method of choice. ZIKV RNA can be detected in urine for some days longer.[22,23] ZIKV is also present in semen for an unknown length of time, and scattered reports of sexual transmission of ZIKV have emerged.[24-28] ZIKV RNA testing is not recommended for pregnant women after the first week after the onset of clinical disease. The diagnosis is usually based on a ZIKV-specific antibody response with higher IgM and neutralizing-antibody responses to ZIKV than to other flaviviruses.[13] However, we have detected ZIKV RNA in the serum of a pregnant woman at 4 weeks and 10 weeks after the clinical onset of ZIKV infection but not after delivery. We suspect that the persistent ZIKV viremia in the patient described here was a consequence of viral replication in the fetus or placenta, which had high viral loads. Therefore, in addition to current ZIKV diagnostics, the use of quantitative RT-PCR methods may be a potential diagnostic approach for ongoing placental or fetal infections in pregnant women. Notably, in this patient, the ZIKV RNA levels were slightly higher in the maternal serum than in the amniotic fluid. The dynamics of ZIKV RNA in the serum of infected pregnant women are not well understood and will need to be assessed in larger studies.

It is estimated that 80% of ZIKV infections are asymptomatic.[29] Although the evidence of the association between the presence of ZIKV in pregnant women and fetal brain abnormalities continues to grow, the timing of infection during fetal development and other factors that may have an effect on viral pathogenesis and their effects on the appearance of brain abnormalities on imaging are poorly understood. Oliveira Melo et al.[9] described two cases of ZIKV intrauterine infection associated with microcephaly and brain calcifications that were diagnosed by means of ultrasonography during the third trimester. Similar to the fetus in our report, the two fetuses in that study showed abnormal development of the corpus callosum and decreased brain parenchymal volume. In the case described by Mlakar et al.,[10] the results of ultrasonography that was performed at 14 weeks and 20 weeks of gestation were normal, but microcephaly, ventriculomegaly, and calcifications were seen on ultrasonography at 29 weeks of gestation.[10] In the larger Brazilian cohort, cerebellar atrophy was seen in a fetus at 20 weeks of gestation, but microcephaly was not diagnosed until 27 to 35 weeks in their cohort.[11] In our study, a review of three sequential ultrasonographic images between 16 and 20 weeks showed a decrease in the fetal head circumferences from the 47th percentile to the 24th percentile, which suggests a reduction in the rate of

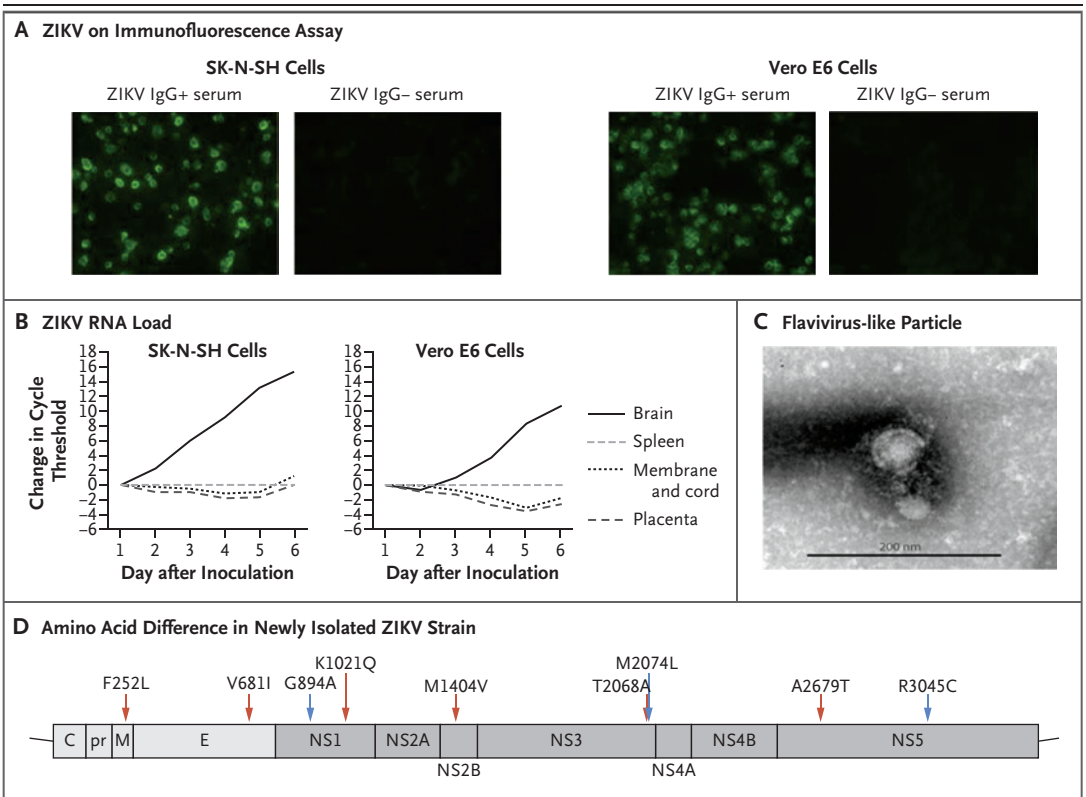

Figure 5. Isolation of ZIKV from Fetal Brain Tissue, ZIKV Growth in Fetal Tissues, Electron Microscopy of a Flavivirus-like Particle, and Amino Acid Differences in the Newly Isolated Strain.

Panel A shows immunofluorescence assays of human neuroblastoma cells (SK-N-SH) and Vero E6 cells that were inoculated with fetal tissue samples to determine the presence of ZIKV. The samples were shown to express ZIKV antigens by reactivity with human convalescent anti-ZIKV serum (ZIKV IgG-positive and IgG-negative [control] samples; dilution, 1:40) obtained from the father. Antihuman IgG fluorescein isothiocyanate conjugate was used as a reagent. Panel B shows the growth curve of ZIKV in SK-N-SH and Vero E6 cells on RT-PCR, indicating the change in ZIKV RNA loads (as determined by the change in cycle threshold) in cell cultures after inoculation with samples from fetal brain, spleen, membrane and cord, and placenta. Panel C shows an electron microscopic image of a particle resembling a flavivirus from supernatant of SK-N-SH cells inoculated with fetal brain tissue. Panel D shows amino acid differences between the FB-GWUH-2016 isolate of ZIKV in this study and the related Guatemalan ZIKV strains (red arrows) and the amino acids that were identical in the study isolate and the related strains but distinct from all other known epidemic strains (blue arrows).

brain growth during that period (Fig. S3 in the Supplementary Appendix). We suspect these reductions in brain growth would have eventually met the criteria for microcephaly. As this case shows, the latency period between ZIKV infection of the fetal brain and the detection of microcephaly and intracranial calcifications on ultrasonography is likely to be prolonged. Negative ultrasonographic studies during this period would be falsely reassuring and might delay critical time-sensitive decision making. Serial ultrasonographic measurements of head circumference may provide useful predictive information. The superior soft-tissue resolution of fetal brain MRI might be more sensitive to developmental and encephaloclastic changes, thereby expediting the detection of evolving fetal brain anomalies.

This case is an early foray into the histopathological findings associated with ZIKV in the midgestational fetal brain. The overwhelming findings were of loss of intermediately differentiated postmigratory neurons through an apoptotic mechanism. There appeared to be preservation of more differentiated neurons in basal ganglia, limbic region, and dorsal spinal cord. The germinal matrix cells also appeared to be spared.

Of note, the germinal matrix consists predominantly of glioblasts at midgestation with the majority of the neuroblasts having already migrated out of the zone. Although we could not evaluate neuronal precursor subtypes other than calretinin-expressing interneuron lineage cells, selective neuronal vulnerability to ZIKV injury requires further investigation.

The successful isolation of infectious ZIKV from human fetal brain fulfills Koch's second postulate regarding the isolation of pathogens from a diseased organism and strengthens the association between congenital ZIKV infection and fetal brain damage. Although ZIKV RNA was found in several fetal organs and the placenta, the virus could be isolated only from brain tissue. The rapid isolation in a human neuroblastoma cell line suggests a predilection of the ZIKV strain for human neural lineage cells. This hypothesis is in line with the histopathological findings and the results of a recent study showing a high rate of ZIKV infection in cortical neural progenitor cells but not in embryonic or pluripotent stem cells.[30] The close genetic relationship between the isolate in our report and Guatemalan ZIKV strains was consistent with the anamnestic knowledge on the likely geographical origin of the infection. We found a relatively high frequency of nonsynonymous mutations between the FB-GWUH-2016 genome and the Guatemalan ZIKV genome (Fig. S4 in the Supplementary Appendix), a finding that could indicate viral adaptation to growth in the fetal brain. However, no amino acid changes were identical to previously reported alterations in the ZIKV genome sequenced from fetal brain tissue.[10]

In conclusion, our study highlights the possible importance of ZIKV RNA testing of serum obtained from pregnant women beyond the first week after symptom onset, as well as a more detailed evaluation of the fetal intracranial anatomy by means of serial fetal ultrasonography or fetal brain MRI. The isolation of ZIKV from fetal brain provides additional evidence for the association between congenital ZIKV infection and fetal brain damage and provides tools for further studies of the pathogenesis of ZIKV-induced microcephaly. Future studies at various gestational ages will offer better insight into the role of ZIKV infection in abnormal brain development and provide markers for its detection.

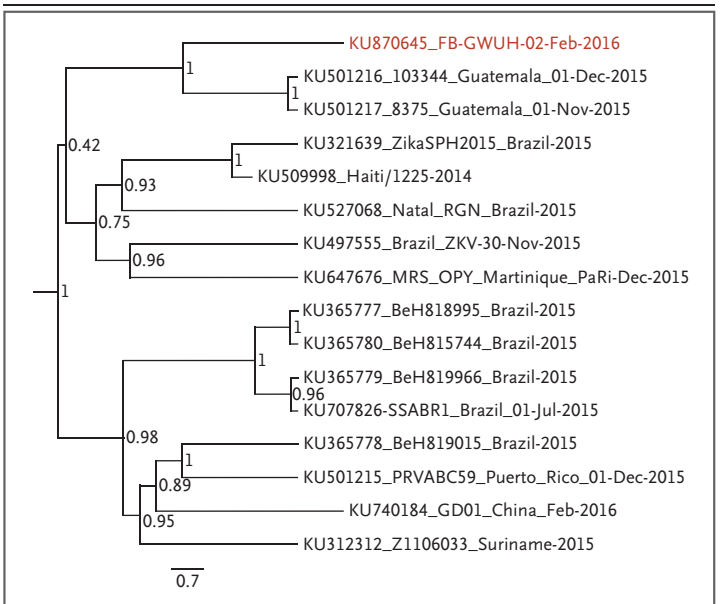

Figure 6. Phylogenetic Tree Showing Newly Isolated ZIKV Strain.

The FB-GWUH-2016 ZIKV strain that was isolated in the fetal brain in this case report is shown at the top of a phylogenetic tree, which was constructed with the use of the Bayesian Markov chain Monte Carlo method. A subclade of Asian lineage that contains the American ZIKV strains is shown. Viral strains are listed according to country and year of collection. The scale bar shows the nucleotide sequence divergence. An expanded phylogenetic tree showing the complete coding regions of ZIKV strains (as of February 28, 2016) is provided in Fig. S6 in the Supplementary Appendix.

Disclosure forms provided by the authors are available with the full text of this article at NEJM.org.

We thank the patient and her husband for their support of our study; Irina Suomalainen, Inkeri Luoto, and Sanna Mäki of the University of Helsinki for their technical assistance; Tamas Baszinka and Kirsi Aaltonen for their help in preparing samples; Dr. Eili Huhtamo for guidance in setting up the nested RT-PCR assay; the Finnish IT Center for Science for the allocation of computational resources; and Yvette Veloso, Mandy Field, and Laurie King for their technical support.

APPENDIX

The authors' full names and academic degrees are as follows: Rita W. Driggers, M.D., Cheng-Ying Ho, M.D., Ph.D., Essi M. Korhonen, M.Sc., Suvi Kuivanen, M.Sc., Anne J. Jääskeläinen, Ph.D., Teemu Smura, Ph.D., Avi Rosenberg, M.D., Ph.D., D. Ashley Hill, M.D., Roberta L. DeBiasi, M.D., Gilbert Vezina, M.D., Julia Timofeev, M.D., Fausto J. Rodriguez, M.D., Lev Levanov, Ph.D., Jennifer Razak, M.G.C., C.G.C, Preetha Iyengar, M.D., Andrew Hennenfent, D.V.M., M.P.H., Richard Kennedy, M.D., Robert Lanciotti, Ph.D., Adre du Plessis, M.B., Ch.B., M.P.H., and Olli Vapalahti, M.D., Ph.D.

The authors' affiliations are as follows: the Department of Gynecology and Obstetrics, Division of Maternal Fetal Medicine (R.W.D., J.T.), and the Department of Pathology (F.J.R.), Johns Hopkins University School of Medicine, Baltimore; the Division of Maternal Fetal

Medicine, Sibley Memorial Hospital (R.W.D., J.T., J.R.), the Division of Pathology and Center for Genetic Medicine Research (C.-Y.H., A.R., D.A.H.), Division of Pediatric Infectious Diseases (R.L.D.), Department of Diagnostic Radiology and Imaging (G.V.), and the Fetal Medicine Institute, Division of Fetal and Transitional Medicine (A.P.), Children's National Health System, the Departments of Integrative Systems Biology (C.-Y.H., D.A.H.), Pediatrics and Microbiology, Immunology and Tropical Medicine (R.L.D.B.), and Radiology and Pediatrics (G.V.), George Washington University School of Medicine and Health Sciences, the Center for Policy, Planning and Evaluation (P.I.) and Centers for Disease Control and Prevention (CDC)–Council of State and Territorial Epidemiologists (CSTE) Applied Epidemiology Fellowship (A.H.), District of Columbia Department of Health, and One Medical Group (R.K.) — all in Washington, DC; the Departments of Virology (E.M.K., S.K., T.S., L.L., O.V.) and Veterinary Biosciences (E.M.K., O.V.), University of Helsinki, and the Department of Virology and Immunology, University of Helsinki and Helsinki University Hospital (A.J.J., O.V.), Helsinki; and the Arboviral Diseases Branch, Division of Vector-Borne Diseases, National Center for Emerging Zoonotic Infectious Diseases, CDC, Atlanta (R.L.).

REFERENCES

1. Dick GW, Kitchen SF, Haddow AJ. Zika virus. I. Isolations and serological specificity. Trans R Soc Trop Med Hyg 1952;46:509-20.
2. Cao-Lormeau VM, Roche C, Teissier A, et al. Zika virus, French Polynesia, South Pacific, 2013. Emerg Infect Dis 2014;20:1085-6.
3. Duffy MR, Chen T-H, Hancock WT, et al. Zika virus outbreak on Yap Island, Federated States of Micronesia. N Engl J Med 2009;360:2536-43.
4. Musso D, Nilles EJ, Cao-Lormeau VM. Rapid spread of emerging Zika virus in the Pacific area. Clin Microbiol Infect 2014;20:O595-6.
5. Zika virus outbreaks in the Americas. Wkly Epidemiol Rec 2015;90:609-10.
6. Lanciotti RS, Kosoy OL, Laven JJ, et al. Genetic and serologic properties of Zika virus associated with an epidemic, Yap State, Micronesia, 2007. Emerg Infect Dis 2008;14:1232-9.
7. Lanciotti RS, Lambert AJ, Holodniy M, Saavedra S, del Carmen Castillo SL. Phylogeny of Zika virus in western hemisphere, 2015. Emerg Infect Dis (in press).
8. Besnard M, Lastere S, Teissier A, Cao-Lormeau V, Musso D. Evidence of perinatal transmission of Zika virus, French Polynesia, December 2013 and February 2014. Euro Surveill 2014;19.
9. Oliveira Melo AS, Malinger G, Ximenes R, Szejnfeld PO, Alves Sampaio S, Bispo de Filippis AM. Zika virus intrauterine infection causes fetal brain abnormality and microcephaly: tip of the iceberg? Ultrasound Obstet Gynecol 2016;47:6-7.
10. Mlakar J, Korva M, Tul N, et al. Zika virus associated with microcephaly. N Engl J Med 2016;374:951-8.
11. Brasil P, Pereira JP Jr, Raja Gabaglia C, et al. Zika virus infection in pregnant women in Rio de Janeiro — preliminary report. N Engl J Med. DOI: 10.1056/NEJMoa1602412.
12. Interim guidelines for pregnant women during a Zika virus outbreak — United States, 2016. MMWR Morb Mortal Wkly Rep 2016;65:30-3.
13. Zika virus infection: global update on epidemiology and potentially associated clinical manifestations. Wkly Epidemiol Rec 2016;91:73-81.
14. Rapid risk assessment: Zika virus epidemic in the Americas: potential association with microcephaly and Guillain-Barre syndrome. Stockholm: European Center for Disease Prevention and Control, 2015.
15. Zika travel information. Atlanta: Centers for Disease Control and Prevention, January 2016 (http://wwwnc.cdc.gov/travel/page/zika-travel-information).
16. Update: interim guidance for health care providers caring for women of reproductive age with possible Zika virus exposure — United States, 2016. MMWR Morb Mortal Wkly Rep 2016 March 25 (http://www.cdc.gov/mmwr/volumes/65/wr/mm6512e2er.htm?s_cid=mm6512e2er).
17. CDC health advisory: recognizing, managing, and reporting Zika virus infections in travelers returning from Central America, South America, the Caribbean and Mexico. Atlanta: Centers for Disease Control and Prevention, 2016 (http://emergency.cdc.gov/han/han00385.asp).
18. Table 24. In: Kline-Fath B, Bahado-Singh R, Bulas DI. Fundamental and advanced fetal imaging: ultrasound and MRI. Philadelphia: Wolters Kluwer Health, 2015:860-3.
19. Harreld JH, Bhore R, Chason DP, Twickler DM. Corpus callosum length by gestational age as evaluated by fetal MR imaging. AJNR Am J Neuroradiol 2011;32:490-4.
20. Means and standard deviations of organ weights and measurements of live-born infants. In: Gilbert-Barness E, Debich-Spicer DE. Handbook of pediatric autopsy pathology. New York: Humana Press, 2005:54.
21. About Zika virus disease. Atlanta: Centers for Disease Control and Prevention, 2016 (http://www.cdc.gov/zika/about/index.html).
22. Gourinat AC, O'Connor O, Calvez E, Goarant C, Dupont-Rouzeyrol M. Detection of Zika virus in urine. Emerg Infect Dis 2015;21:84-6.
23. Korhonen EM, Huhtamo E, Smura T, Kallio-Kokko H, Raassina M, Vapalahti O. Zika virus infection in a traveller returning from the Maldives, June 2015. Euro Surveill 2016;21.
24. Musso D, Roche C, Robin E, Nhan T, Teissier A, Cao-Lormeau VM. Potential sexual transmission of Zika virus. Emerg Infect Dis 2015;21:359-61.
25. Foy BD, Kobylinski KC, Chilson Foy JL, et al. Probable non-vector-borne transmission of Zika virus, Colorado, USA. Emerg Infect Dis 2011;17:880-2.
26. McCarthy M. Zika virus was transmitted by sexual contact in Texas, health officials report. BMJ 2016;352:i720.
27. Venturi G, Zammarchi L, Fortuna C, et al. An autochthonous case of Zika due to possible sexual transmission, Florence, Italy, 2014. Euro Surveill 2016;21.
28. Transmission of Zika virus through sexual contact with travelers to areas of ongoing transmission — continental United States, 2016. MMWR Morb Mortal Wkly Rep 2016;65:215-6.
29. Zika virus: clinical evaluation and disease. Atlanta: Centers for Disease Control and Prevention (http://www.cdc.gov/zika/hc-providers/clinicalevaluation.html).
30. Tang H, Hammack C, Ogden SC, et al. Zika virus infects human cortical neural progenitors and attenuates their growth. Cell Stem Cell 2016 March 3 (Epub ahead of print).